Materials Letters 275 (2020) 128076

Contents lists available at ScienceDirect

Materials Letters

journal homepage: www.elsevier.com/locate/mlblue

The influence of $MoSe_2$ coated onto Pt film to DSSC performance with the structure TiO_2/Dye/L_xMoSe_2Pt ($0 \leq x \leq 5$)

Marjoni Imamora Ali Umar [a,*], Resti [a], Venny Haris [a], Akrajas Ali Umar [b]

[a] Department of Physics Education, Faculty Tarbiyah and Teacher Training (FTIK), IAIN Batusangkar, 27213, Batusangkar, Tanah Datar, West-Sumatera, Indonesia
[b] Institute Microengineering and Nanoelectronic (IMEN), Universiti Kebangsaan Malaysia, Bangi, Selangor Darul Ehsan, Malaysia

ARTICLE INFO

Article history:
Received 10 May 2020
Received in revised form 18 May 2020
Accepted 29 May 2020
Available online 1 June 2020

Keywords:
Counter-electrode
Semiconductors
L_xMoSe_2Pt
$MoSe_2$
DSSC-performance

ABSTRACT

Research on the influence of Molybdenum Diselenide ($MoSe_2$) coating on platinum (Pt) to performing dye-sensitized solar cell (DSSC) with the structure of TiO_2/Dye/L_xMoSe_2Pt, ($0 \leq x \leq 5$) is reported. The hydrothermal method has successfully synthesized the TiO_2 film with square and porous morphology on the indium titanium oxide (ITO) surface. Four peaks of the Raman Scattering detected from the semiconductor confirm the formation of TiO_2 film. The liquid-phase deposition (LPD) also successfully prepared the Pt film. Onto the prepared Pt, the $MoSe_2$ was coated to produce L_xMoSe_2Pt ($0 \leq x \leq 5$) and then use them as the counter electrode (CE). The best DSSC devices with TiO_2/Dye/L_2MoSe_2Pt structures have resulted in current–density, Voc, and solar cell performance of 11.204 mA/cm^2, 0.66 V, and 2.967%, respectively. The Bode graph confirmed this device has the longest lifetime, proven by the highest peak rise in the lowest frequency. Besides, high-frequency also shows the device has low resistance, useful for accelerating the electrons flow and enhancing DSSC performance.

1. Introduction

DSSC is a solar device with semiconductor-based which determined by the effectiveness of the photo-physiochemical phenomenon on the semiconductor [1]. As a third-generation solar-cell has several advantages, such as cheaper, simple-production, and high-efficiency [2]. We believe the efficiency might be enhanced by modifying the key components of the DSSC, such as semiconductor, CE, and electrolyte. Semiconductors which have wide band-gap energy such as TiO_2 [3] with the sense of dye-sensitized material, and the CE with high electro-catalytic, good conductivity and stable [2] could further improve the DSSC performance.

Pt is a popular CE in DSSC application due to it has high efficiency [4,5] compared to Carbon and Graphene [6–18]. However, an effort to further enhance the Pt properties by adding or attach them to other materials has been reported. For instance, Graphene (G-Pt) and reduced graphene oxide/rGO (rGO-Pt), resulting in the efficiency increased around 0.8% and 0.9%, respectively [19]. Besides, Gong et al. added one-layer of Pt on Graphene (GNS) [6], resulting in the efficiency increased from 4.76% (Pt) to 6.09% (GNS/Pt). Besides, Cheng et al. also reported the MoS_2 addition (Pt/MoS_2) producing the device performance increase of 0.6% [20]. In this research, we report the use of $MoSe_2$ as a coated layer on platinum and then used them as a CE on the DSSC device. Since it has a very active electrocatalytic, good conductivity [21] and resistant to corrosion caused by electrolytes [22]. The best performance obtained is 2.967% with the V_{OC} and fill-factor generated by 0.66 V and 40.11%, respectively.

2. Material and methods

2.1. Synthesis TiO_2 and Pt + $MoSe_2$ (L_xMoSe_2Pt, $0 \leq x \leq 5$)

We purchased all chemicals in this work from Sigma-Aldrich. We synthesized TiO_2 semiconductor on the ITO substrate by using a growth solution which consists of 5 mL Ammonium-Hexafluorotitanate and 5 mL boric acid with deionized (DI) water. The detail of the synthesis process has been well-explained in the previous report [3]. Pt films were synthesized using the LPD method on the ITO substrate. We started the Pt synthesis from seeding 3 times by using a solution of L-Ascorbic Acid and potassium tetrachloroplatinate (K_2PtCl_4) with a temperature of 50 °C for 2 h. After that, we continued to Pt growth, using a solution of K_2PtCl_4, L-Ascorbic Acid, Polyvinyl pyrrolidone, and natrium hydroxide with a temperature of 50 °C for 5 h. Last, the prepared Pt was then annealed in an oven for 1 h at 250 °C. Next, the

* Corresponding author.
E-mail address: marjoni.imamora@iainbatusangkar.ac.id (M.I. Ali Umar).

https://doi.org/10.1016/j.matlet.2020.128076
0167-577X/

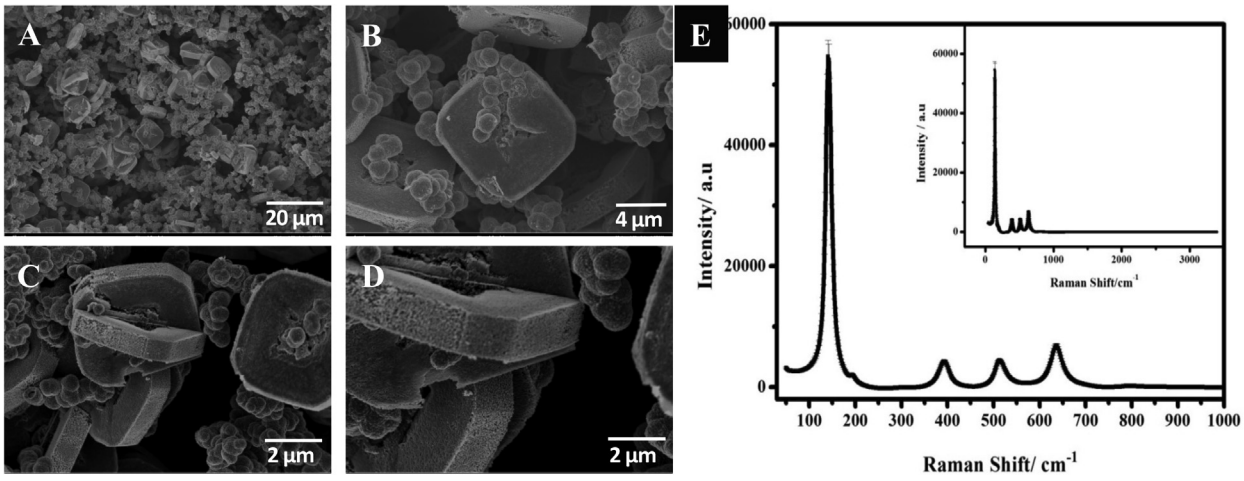

Fig. 1. A-D) are the FESEM image of a TiO_2 semiconductor film, and E) The Raman Scattering Spectra of TiO_2.

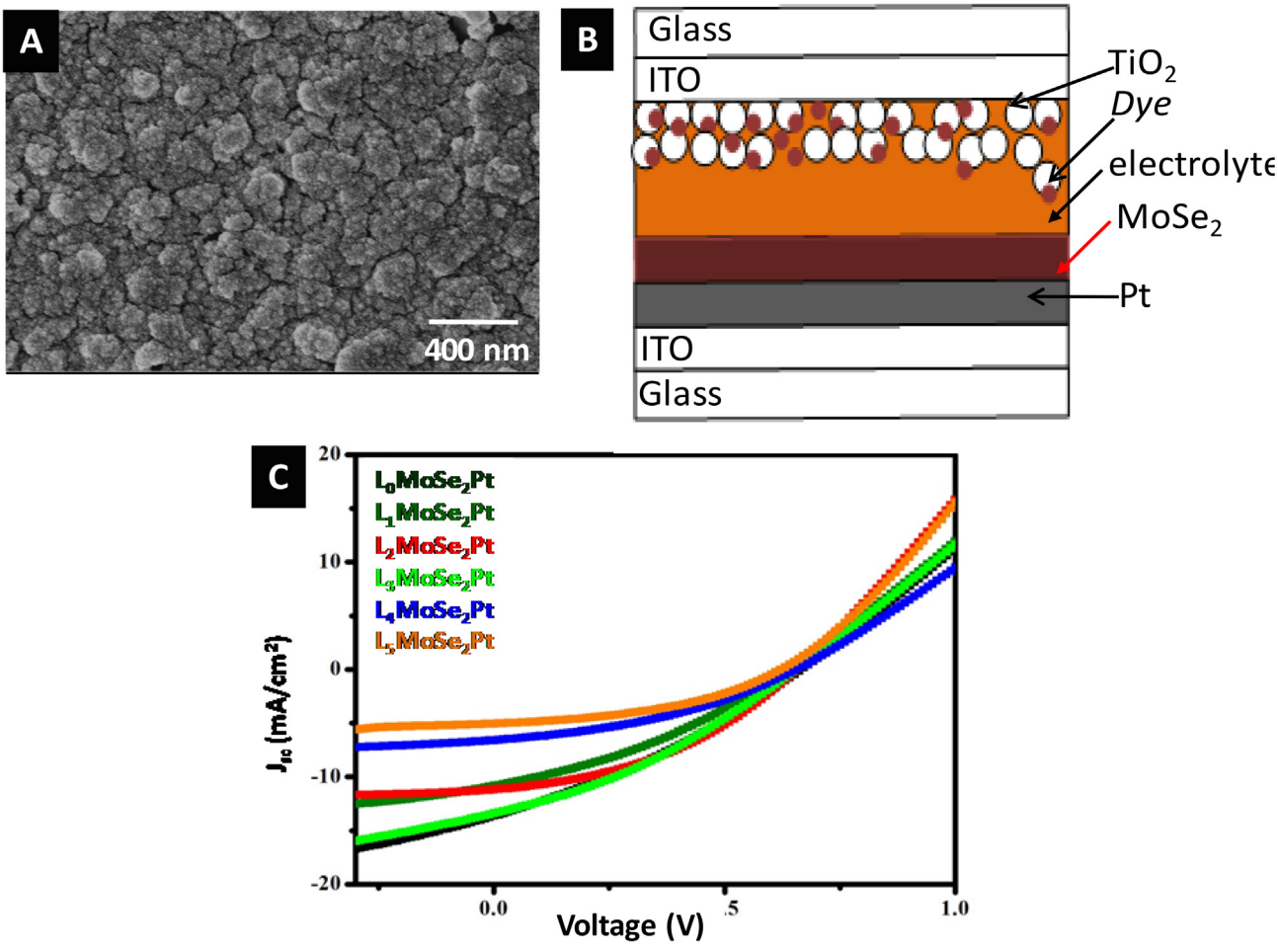

Fig. 2. A). The FESEM image of Pt film (magnification of 50,000 times), B). DSSC array with the $MoSe_2$ coating. C). The J-V curve of DSSC devices with the structure TiO_2/Dye/L_xMoSe_2Pt ($0 \leq x \leq 5$).

resultant Pt was coated by $MoSe_2$, forming the L_xMoSe_2Pt ($0 \leq x \leq 5$) film using the LPD method. The Pt film was put into the growth-solution (0.5 M of Hexamethylenetetramine 0.5 M, 0.05 M of Ammonium Tetrathromolybdate, 0.1 M of Sodium Borohydrate and 0.01 M of Selenium) and synthesized using water-bath at 90 °C for 30 min. We repeated these steps to produce two until five layers of $MoSe_2$. Last, the coated Pt was annealed by hydrogen flow at 300 °C for 3 h. During the synthesis process, the morphology of TiO_2 and Platinum film was observed with a FESEM and Raman Scattering as well.

2.2. Preparation of DSSC devices with the structured of TiO_2/Dye/L_xMoSe_2Pt ($0 \leq x \leq 5$)

We designed DSSC devices as Fig. 2B to see the influence of L_xMoSe_2Pt ($0 \leq x \leq 5$) film as a CE on the device performance. The TiO_2 semiconductor as a photoanode is assembled (after immersed in dye solution (0.05 mM N719) at room temperature for 15 h) with a CE using a metal clamp. A para-film with a circle hole of 0.23 cm^2 was sandwiched between the TiO_2 and the L_x-$MoSe_2Pt$ and injected the electrolyte solution. Last, the current-voltage (J-V) curve of the DSSC was obtained using the Gamry instrument under illumination by simulated sunlight with an intensity of 100 mW cm^2 to characterize the device performance.

3. Results and discussion

FESEM image shows the synthesized TiO_2 successfully covered the entire ITO surface (see Fig. 1A). The TiO_2 particles have a morphology that resembles a square shape (Fig. 1B, C) with porous structures and varying particle sizes (see Fig. 1C and D). The porous structure is believed caused by the use of high temperatures during the growth process. This condition is useful to absorb more dye and enhanced DSSC performance [3]. Fig. 1E shows the Raman Scattering spectrum consisting of 4 peaks of 141 cm^{-1}, 393 cm^{-1}, 513 cm^{-1}, and 636 cm^{-1} with one peak having high intensity between 100 and 800 cm^{-1}. The resultant peaks are comparable with the research results of Tian et al. [23] and confirm the formation of TiO_2.

Fig. 2A is the FESEM image of Pt with asymmetrical structures (particle size of 156 ± 16 nm) and covers the entire ITO surface. Next, the synthesized L_xMoSe_2Pt ($0 \leq x \leq 5$) was used as CE in DSSC devices with the structured TiO_2/Dye/L_xMoSe_2Pt (see Fig. 2B). The J-V curve of DSSC and the photovoltaic parameter are described in Fig. 2C and Table 1, respectively. From the Table 1 shows the DSSC performance start from 2.858%, and then decreased to 2.364% when using L_1MoSe_2Pt as CE. We believed, it occurred as an effect of the heating repetition during $MoSe_2$ coating, and causing the Pt structure damaged and reduced film adhesion [24]. Interestingly, the DSSC performance increase when using the L_2MoSe2Pt as CE to 2.967%. In this stage the $MoSe_2$ coating rather thick, and covering the Pt structure from directly exposed to high temperature, improving the surface area and their conductivity [6]. Besides, the increasing of the surface area providing sensitization of dye materials, speed-up the electrolyte redox reaction [25], and producing higher performance [26]. Then, the DSSC performance decrease again with the number of $MoSe_2$ coating layer increased (L_3MoSe_2Pt, L_4MoSe_2Pt, and L_5MoSe_2Pt). Besides the previous reason, since the addition of each layer of $MoSe_2$ does not followed by the annealed process, causing the bond between them still fragile and easily damaged also causing this phenomenon. The best DSSC performance shows 0.11% higher than the first devices and confirming the coated of $MoSe_2$ are successfully catalyst the Pt film [2,27]. Since the TiO_2, dye-materials [16,18], and electrolyte-selection are far from being optimized, applying the Pt in optimized device will enhanced the DSSC performance. These results also support by Bode graphs (see Fig. 3) which shows that this device produces the highest peak on the lowest frequency. Its means, high-frequency peaks show the device has small resistance and highest lifetime compared to other [28]. Besides, the small resistance leading to speed-up the flow of electrons [25], and producing the DSSC devices with the higher performance [29].

Table 1
The photovoltaic parameters of DSSC device with the structure TiO_2/Dye/L_xMoSe_2Pt ($0 \leq x \leq 5$).

CE	Voc (V)	Jsc (mA/cm^2)	FF (%)	Eff (%)
L_0MoSe_2Pt	0.67	13.635	31.26	2.858
L_1MoSe_2Pt	0.65	10.861	33.47	2.364
L_2MoSe2Pt	0.66	11.204	40.11	2.967
L_3MoSe_2Pt	0.66	13.426	32.92	2.921
L_4MoSe_2Pt	0.66	6.600	37.67	1.644
L_5MoSe_2Pt	0.63	5.078	42.13	1.350

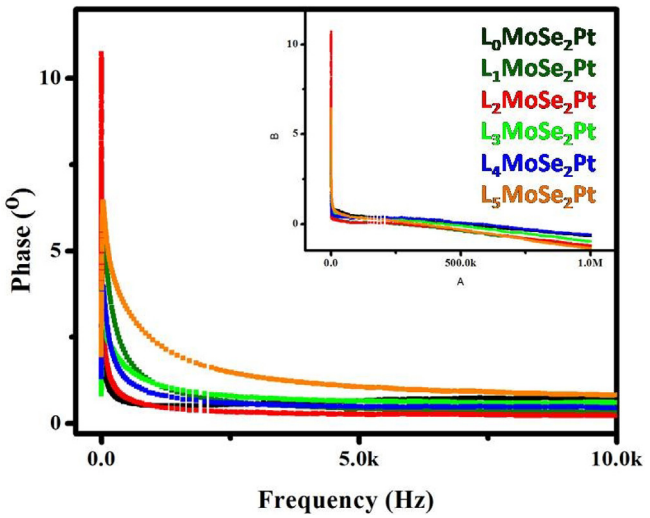

Fig. 3. Bode graphics of 6 DSSC devices with structure TiO_2/Dye/L_xMoSe_2Pt ($0 \leq x \leq 5$).

4. Conclusion

The influence of $MoSe_2$ coated onto Pt film to produce L_xMoSe_2-Pt ($0 \leq x \leq 5$) as CE on the DSSC performance has been carried out. The best DSSC devices with the structure of TiO_2/Dye/L_2MoSe_2Pt have resulted in current density, Voc, and solar cell performance of 11.204 mA/cm^2, 0.66 V, and 2.967%, respectively. Bode graph confirming the device structure has the highest lifetime because of the highest peak is detected on the lowest frequency. Besides, the high-frequency peaks also show small device resistance, leading to accelerating the electrons flow and enhanced DSSC performance.

CRediT authorship contribution statement

Marjoni Imamora Ali Umar: Conceptualization, Methodology, Writing - original draft, Writing - review & editing. **Resti:** Investigation, Writing - original draft. **Venny Haris:** Investigation, Validation. **Akrajas Ali Umar:** Supervision, Conceptualization, Methodology, Writing - review & editing.

Declaration of Competing Interest

The authors declare that they have no known competing financial interests or personal relationships that could have appeared to influence the work reported in this paper.

Acknowledgments

We would like to thank the MOHE Malaysia, Dr. H. Kasmuri, M. A. (Rector), Dr. Sirajul Munir, M.Pd. (Dean), and Bundo Hj. Cherana, Fitri Yenni, M.Sc, Miftahul Farid Rafi M.I, and Cresvo Fourvindra Pratama for their contribution to this work.

References

[1] A.A. Umar, S. Nafisah, S.K.M. Saad, S.T. Tan, A. Balouch, M.M. Salleh, M. Oyama, Poriferous microtablet of anatase TiO2 growth on an ITO surface for high-efficiency dye-sensitized solar cells, Sol. Energy Mater. Sol. cells 122 (2014) 174–182.

[2] J. Dong, J. Wu, J. Jia, L. Hu, S. Dai, Cobalt/molybdenum ternary hybrid with hierarchical architecture used as high efficient counter electrode for dye-sensitized solar cells, Sol. Energy 122 (2015) 326–333.

[3] A.A. Umar, S.K.M. Saad, M.I.A. Umar, M.Y.A. Rahman, M. Oyama, Advances in porous and high-energy (001)-faceted anatase TiO2 nanostructures, Opt. Mater. 75 (2018) 390–430.

[4] P. Poudel, A. Thapa, H. Elbohy, Q. Qiao, Improved performance of dye solar cells using nanocarbon as support for platinum nanoparticles in counter electrode, Nano Energy 5 (2014) 116–121.

[5] A. Iefanova, J. Nepal, P. Poudel, D. Davoux, U. Gautam, V. Mallam, Q. Qiao, B. Logue, M.F. Baroughi, Transparent platinum counter electrode for efficient semi-transparent dye-sensitized solar cells, Thin Solid Films 562 (2014) 578–584.

[6] F. Gong, H. Wang, Z.-S. Wang, Self-assembled monolayer of graphene/Pt as counter electrode for efficient dye-sensitized solar cell, Phys. Chem. Chem. Phys. 13 (39) (2011) 17676–17682.

[7] M.I. Ali Umar, C.C. Yap, R. Awang, A. Ali Umar, M. Mat Salleh, M. Yahaya, Formation of gold-coated multilayer graphene via thermal reduction, Mater. Lett. 106 (2013) 200–203.

[8] L.-L. Li, C.-W. Chang, H.-H. Wu, J.-W. Shiu, P.-T. Wu, E.W.-G. Diau, Morphological control of platinum nanostructures for highly efficient dye-sensitized solar cells, J. Mater. Chem. 22 (13) (2012) 6267–6273.

[9] J. Gong, Z. Zhou, K. Sumathy, H. Yang, Q. Qiao, Activated graphene nanoplatelets as a counter electrode for dye-sensitized solar cells, J. Appl. Phys. 119 (13) (2016) 135501.

[10] A. Aboagye, H. Elbohy, A.D. Kelkar, Q. Qiao, J. Zai, X. Qian, L. Zhang, Electrospun carbon nanofibers with surface-attached platinum nanoparticles as cost-effective and efficient counter electrode for dye-sensitized solar cells, Nano Energy 11 (2015) 550–556.

[11] P. Poudel, Q. Qiao, Carbon nanostructure counter electrodes for low cost and stable dye-sensitized solar cells, Nano Energy 4 (2014) 157–175.

[12] Z. Zhou, S. Sigdel, J. Gong, B. Vaagensmith, H. Elbohy, H. Yang, S. Krishnan, X.-F. Wu, Q. Qiao, Graphene-beaded carbon nanofibers with incorporated Ni nanoparticles as efficient counter-electrode for dye-sensitized solar cells, Nano Energy 22 (2016) 558–563.

[13] P. Poudel, L. Zhang, P. Joshi, S. Venkatesan, H. Fong, Q. Qiao, Enhanced performance in dye-sensitized solar cells via carbon nanofibers–platinum composite counter electrodes, Nanoscale 4 (15) (2012) 4726–4730.

[14] Y. Zhao, A. Thapa, Q. Feng, M. Xi, Q. Qiao, H. Fong, Electrospun TiC/C nano-felt surface-decorated with Pt nanoparticles as highly efficient and cost-effective counter electrode for dye-sensitized solar cells, Nanoscale 5 (23) (2013) 11742–11747.

[15] X. Ma, H. Elbohy, S. Sigdel, C. Lai, Q. Qiao, H. Fong, Electrospun carbon nano-felt derived from alkali lignin for cost-effective counter electrodes of dye-sensitized solar cells, RSC Adv. 6 (14) (2016) 11481–11487.

[16] Q. He, S. Huang, J. Zai, N. Tang, B. Li, Q. Qiao, X. Qian, Efficient counter electrode manufactured from Ag2S nanocrystal ink for dye-sensitized solar cells, Chem.–A Eur. J. 21 (43) (2015) 15153–15157.

[17] Q. He, S. Huang, C. Wang, Q. Qiao, N. Liang, M. Xu, W. Chen, J. Zai, X. Qian, The role of Mott-Schottky heterojunctions in Ag–Ag8SnS6 as counter electrodes in dye-sensitized solar cells, ChemSusChem 8 (5) (2015) 817–820.

[18] Q. He, T. Qian, J. Zai, Q. Qiao, S. Huang, Y. Li, M. Wang, Efficient Ag 8 GeS 6 counter electrode prepared from nanocrystal ink for dye-sensitized solar cells, J. Mater. Chem. A 3 (40) (2015) 20359–20365.

[19] R. Bajpai, S. Roy, P. Kumar, P. Bajpai, N. Kulshrestha, J. Rafiee, N. Koratkar, D. Misra, Graphene supported platinum nanoparticle counter-electrode for enhanced performance of dye-sensitized solar cells, ACS Appl. Mater. Interfaces 3 (10) (2011) 3884–3889.

[20] C.-K. Cheng, J.-Y. Lin, K.-C. Huang, T.-K. Yeh, C.-K. Hsieh, Enhanced efficiency of dye-sensitized solar counter electrodes consisting of two-dimensional nanostructural molybdenum disulfide nanosheets supported Pt nanoparticles, Coat. 7 (10) (2017) 167.

[21] Y. Huang, H. Lu, H. Gu, J. Fu, S. Mo, C. Wei, Y.-E. Miao, T. Liu, A CNT@ MoSe 2 hybrid catalyst for efficient and stable hydrogen evolution, Nanoscale 7 (44) (2015) 18595–18602.

[22] N. Jena, A. De Sarkar, Compressive strain induced enhancement in thermoelectric-power-factor in monolayer MoS2 nanosheet, J. Phys. Condens. Matter 29 (22) (2017) 225501.

[23] F. Tian, Y. Zhang, J. Zhang, C. Pan, Raman spectroscopy: a new approach to measure the percentage of anatase TiO2 exposed (001) facets, J. Phys. Chem. C 116 (13) (2012) 7515–7519.

[24] Y.L.F. Musico, C.M. Santos, M.L.P. Dalida, D.F. Rodrigues, Improved removal of lead (II) from water using a polymer-based graphene oxide nanocomposite, J. Mater. Chem. A 1 (11) (2013) 3789–3796.

[25] G. Yue, J. Wu, Y. Xiao, M. Huang, J. Lin, J.-Y. Lin, High performance platinum-free counter electrode of molybdenum sulfide–carbon used in dye-sensitized solar cells, J. Mater. Chem. A 1 (4) (2013) 1495–1501.

[26] M.I.A. Umar, F.Y. Naumar, M.M. Salleh, A.A. Umar, Hydrothermally grown of well-aligned ZnONRs: dependence of alignment ordering upon precursor concentration, J. Mater. Sci-Mater. El. 29 (8) (2018) 6892–6897.

[27] A. Abderrahmane, P. Ko, T. Thu, S. Ishizawa, T. Takamura, A. Sandhu, High photosensitivity few-layered MoSe2 back-gated field-effect phototransistors, Nanotechnology 25 (36) (2014) 365202.

[28] A. Lim, N. Haji Manaf, K. Tennakoon, R. Chandrakanthi, L.B.L. Lim, J. Bandara, P. Ekanayake, Higher performance of DSSC with dyes from Cladophora sp. as mixed cosensitizer through synergistic effect, J. Biophys. (2015 (2015).).

[29] T. Sawatsuk, A. Chindaduang, C. Sae-Kung, S. Pratontep, G. Tumcharern, Dye-sensitized solar cells based on TiO2–MWCNTs composite electrodes: performance improvement and their mechanisms, Diamond Relat. Mater. 18 (2–3) (2009) 524–527.